Bioorganic & Medicinal Chemistry Letters 22 (2012) 4745–4749

Contents lists available at SciVerse ScienceDirect

Bioorganic & Medicinal Chemistry Letters

journal homepage: www.elsevier.com/locate/bmcl

Synthesis and evaluation of novel F-18 labeled 4-aminoquinazoline derivatives: Potential PET imaging agents for tumor detection

Yurong Chen, Man Feng, Shilei Li, Jingli Xu, Hongyu Ning, Yong He, Xiao Wang, Rui Ding, Chuanmin Qi *

Key laboratory of Radiopharmaceuticals, Ministry of Education, College of Chemistry, Beijing Normal University, Beijing 100875, People's Republic of China

ARTICLE INFO

Article history:
Received 14 February 2012
Revised 9 May 2012
Accepted 18 May 2012
Available online 24 May 2012

Keywords:
^{18}F-labeled
4-Aminoquinazoline derivatives
Tumor detection
PET imaging agent

ABSTRACT

Three novel ^{18}F-labeled 4-aminoquinazoline derivatives, *N*-(3-chloro-4-fluorophenyl)-6-(2-[^{18}F]fluoroethoxy)-7-methoxyquinazolin-4-amine([^{18}F]**1**), *N*-(3-ethynylphenyl)-6-(2-[^{18}F]fluoroethoxy)-7-methoxyquinazolin-4-amine([^{18}F]**2**), and *N*-(3-bromophenyl)-6-(2-[^{18}F]fluoroethoxy)-7-methoxyquinazolin-4-amine([^{18}F]**3**) were synthesized and radiolabeled by two-step reaction with overall radiochemical yield of 21–24% (without decay corrected). Then we carried out their biodistribution experiments in S180 tumor-bearing mice. Results showed that they had certain concentration accumulation in tumor and fast clearance from muscle and blood. It was encouraging that [^{18}F]**3** was competitive among three ^{18}F-labeled 4-aminoquinazoline derivatives in some aspects such as tumor/muscle uptake ratio reaching 7.70 at 60 min post-injection, tumor/blood uptake ratio reaching 6.61 at 120 min post-injection. So we compared radioactivity characteristics of [^{18}F]**3** with those of [^{18}F]-FDG and L-[^{18}F]-FET in the same animal model. The absolute radioactivity uptake of [^{18}F]**3** in tumor reached 3.31 at 60 min p.i., which was slightly higher than [^{18}F]-FDG (2.16) and L-[^{18}F]-FET (2.75) at the same time phase. For [^{18}F]**3**, tumor/muscle uptake ratio peaked 7.70 at 60 min, which was obviously superior to those of [^{18}F]-FDG and L-[^{18}F]-FET at all time points. The tumor/brain uptake ratios of [^{18}F]**3** were 10.36, 17.42, 41.11 at 30 min, 60 min and 120 min post-injection, respectively, and are much higher than those of L-[^{18}F] FET (2.54, 2.92 and 2.95) and [^{18}F]-FDG (0.61, 1.02 and 1.33) at the same time points. All these results indicate that [^{18}F]**3** is promising to become a potential PET tumor imaging agent.

As a class of heterocyclic compounds, aminoquinazolines and their derivatives have many biological activities, such as anti-inflammatory,[1] antibacterial,[2] antiviral[3] and most importantly, anticancer activity.[4,5] And it is the anticancer activity that makes aminoquinazolines derivatives as one important pharmacophore widely used in the developing novel anticancer drugs. Representative drugs, like gefitinib, erlotinib, and lapatinib, have been approved by the FDA and were successfully applied in clinic for the treatment of multiple cancers, such as non-small cell lung cancer,[6,7] pancreatic cancer,[7] breast cancer,[8] etc.

PET is a functional imaging technology which allows the three-dimensional, quantitative determination of the distribution of radioactivity within the human body at a molecular level, both in healthy and pathological states.[9] Of all commonly used positron radionuclides in PET, ^{18}F is often referred to as the 'radionuclide of choice' due to its favorable physical half-life ($t_{1/2}$ = 110 min).[10] It is well known that [^{18}F]-FDG has been the most widely used in clinical diagnoses as PET radiopharmaceutical. However, some drawbacks are found in [^{18}F]-FDG: high uptake in nonmalignant, inflammatory tissues causes false-positive results and high background uptake in normal brain tissues limits its application in brain tumor PET imaging.[11,12] Therefore, there has been a lot of research on the development of novel PET radiotracers,[13,14] for example, L-[^{18}F]-FET,[15] as alternate radiotracer.

Aminoquinazolines and their derivatives are also used for the potential tumor imaging tracers due to inhibiting proliferation of tumor cells.[16–18] So there has been a growing interest in the study of 4-aminoquinazoline drugs in clinical and preclinical trials as tumor imaging tracers via nuclear medicine modality positron emission tomography (PET). The first drug candidates, PD 153035 and its analogues were radiolabeled with [^{11}C]/[^{125}I] and evaluated.[17,18] But the research is still not sufficient.[19,20] Subsequently, several 4-anilinoquinazoline drugs are radiolabeled for PET imaging tracers.[21–23] They include [^{18}F]gefitinib,[24,25] [^{11}C]erlotinib,[26] [^{11}C]-ML03,[27] [^{11}C]/[^{18}F]-ML04.[28,29] 4-aminoquinazoline derivatives as PET imaging tracers have already been developed, but these existing tracers present some drawbacks: low tumor uptake, low solubility and poor stability in vivo.[23,27]

Consequently, we are interested in 4-aminoquinazoline derivatives as PET tracers for tumor diagnose, and we also have been trying to design and develop novel ^{18}F labeled radiotracers for PET imaging. It is reported that the 6- and 7-positions of 4-aminoquinazolinos are very tolerant of substitution, which are preferably

* Corresponding author.
E-mail address: qicmin@sohu.com (C. Qi).

0960-894X/$ - see front matter © 2012 Elsevier Ltd. All rights reserved.
http://dx.doi.org/10.1016/j.bmcl.2012.05.069

electron-donating ethers, and introducing substituent in these positions will enhance their bioactivities.[30] In order to find more appropriate imaging agents overcoming shortcomings mentioned, we designed and synthesized three novel ^{18}F labeled 4-aminoquinazoline derivatives modified by ethylene glycol-1, 2-ditosylate. In this Letter, we described radiosynthesis and preliminarily biological evaluation of three new ^{18}F-labeled radiotracers, *N*-(3-chloro-4-fluorophenyl)-6-(2-[^{18}F]fluoroethoxy)-7-methoxyquinazolin-4-amine([^{18}F]**1**), *N*-(3-ethynylphenyl)-6-(2-[^{18}F]fluoroethoxy)-7-methoxyquinazolin-4-amine([^{18}F]**2**) and *N*-(3-bromophenyl)-6-(2-[^{18}F]fluoroethoxy)-7-methoxyquinazolin-4-amine([^{18}F]**3**) (Fig. 1). Moreover, biological activities of these new compounds were made further evaluation in comparison with [^{18}F]-FDG and L-[^{18}F]-FET.

Compound **11** was synthesized from 3,4-dimethoxybenzoic as shown in Scheme 1 according to procedure in the literature, with slight modification.[31,32] The synthesis routes of compounds **12–17** were a slight modification of the procedures described literature.[32–34] Briefly, Compounds **12, 13** and **14** were prepared through coupling of intermediate **11** with 3-chloro-4-fluoroaniline, 3-bromoaniline and 3-aminophenylacetylene in isopropanol with 85%–96% yield. Hydrolysis of the acetyl group on compounds **12**, **13** and **14** was performed using sodium hydroxide in methanol to give 4-anilino-6-hydroxy-7-methoxyquinazoline derivatives **15**, **16** and **17** in 65%–75% yield. Fluorine-19 substituted compounds [^{19}F]**1**, [^{19}F]**2** and [^{19}F]**3** were synthesized by, respectively, reacting **15**, **16**, and **17** with 1-bromo-2-fluoroethane using potassium carbonate as a base in *N*,*N*-dimethylformamide with 60%–75% yields based on the following procedure in Scheme 1. 2-fluoroethyltosylate (**19**) was synthesized by reacting 1,2-bistosyloxyethane (**18**) with tetrabutylammonium fluoride in acetonitrile in 80% yield. (Scheme 1)

All ^{18}F labeled compounds, [^{18}F]**1**, [^{18}F]**2** and [^{18}F]**3** were prepared with [^{18}F]KF-$K_{2.2.2}$ complex via a prosthetic group in two-step reaction that consisted of ^{18}F-fluorination of ethylene glycol-1, 2-ditosylate and subsequent ^{18}F-fluoroethylation of precursors (Scheme 2). Firstly, 2-[^{18}F]fluoroethyl tosylate (**20**) was prepared by nucleophilic fluorination substitution of compound **18** with anhydrous [^{18}F]KF-cryptate ([$K_{2.2.2}$]/^{18}F) in the presence of acetonitrile at 100 °C for 15 min. Secondly, after acetonitrile was removed at 100 °C under a flow of nitrogen, intermediate **20** without isolation was added to a solution of potassium salt of precursors in DMSO, heating up 100 °C for 15 min, producing ^{18}F-labeled product [^{18}F]**1**, [^{18}F]**2** and [^{18}F]**3**, respectively. The resulting mixture was highly diluted with water, concentrated on a C18 Sep-Pak cartridge and almost quantitatively desorbed with acetonitrile. Following purification was executed by semi-preparative HPLC with reversed-phase Grace Alltima™ C18 Column (250 × 10 mm, particle size: 10 μm). The column was eluted using isocratic solvent as followed Table 1. The eluent was collected, solvent was evaporated and then the products were dissolved in phosphate-buffered saline solution (pH 7.4) for further use. The radiochemical purity and chemical purity were above 99%. The total reaction time for each [^{18}F]-labeled product was about 60 min including purification with radio-HPLC. The overall radiochemical yield without decay correction and retention time were summarized in Table 1.

Partition coefficient was measured using the method which was reported by our team previously.[35] The partition coefficient (log*P*) values of these compounds, [^{18}F]**1**, [^{18}F]**2** and [^{18}F]**3**, were 0.39, 1.64 and 0.89, respectively.

To evaluate stability in plasma of each ^{18}F-labeled radiotracer, 0.1 mL PBS (pH 7.4) solution as described above was added in 2 mL mouse plasma and incubated 2 h at 37 °C. Then acetonitrile was added to plasma solution, and centrifuged to discard plasma proteins. The supernatant part was injected into HPLC to determine the stability of each compound. The results of radio-HPLC analysis suggested that three ^{18}F-labled radiotracers were stable in plasma. In addition, radio-HPLC analysis proved that three ^{18}F-labled radiotracers in saline remained stable in rt and 60 °C for 2 h.

All animal experiments were carried out under humane conditions and in compliance with the national laws related to the conduct of animal experimentation. The biological evaluation studies were investigated in S180 tumor-bearing mice. S180 tumor model was established by injecting 5×10^6 S180 tumor cells into left forelimb of female mice without anesthesia. The experimental procedure was performed after inoculating the tumor cells for 14–18 days when the tumors were about 0.5 cm in diameter. A volume of 0.1 mL ^{18}F labeled radiotracer (8–10 μCi) in a solution of PBS (pH 7.4) purified by radio-HPLC as mentioned above was injected into each mouse through tail vein (4 animals in per time phase). Then the mice were sacrificed at 5, 30, 60 and 120 min post-injection. Tumor, brain, blood, and other organs of interest were collected, wet-weighed, and measured for radioactivity in gamma counter. The biodistribution results of ^{18}F labeled compounds [^{18}F]**1**, [^{18}F]**2** and [^{18}F]**3** were shown in Tables 2–4, respectively. The data in tables was expressed as percentage of injected dose per gram of tissue weight (%ID/g). Values were expressed as mean ± SD (n = 4).

Table 2 presented a rapid distribution of [^{18}F]1 in all organs and tissues. Initial radioactivity uptakes in liver and kidney were high, however, declined rapidly as time lapsed, showed that the systemic metabolism was governed by liver and kidney. Although the radioactivity uptake of [^{18}F]1 in tumor was comparably low at initial time, it had a significant increasing accumulation in tumor from 5 to 120 min post-injection. And maximum of radioactivity uptake in tumor was 5.80 ± 0.72%ID/g at 30 min post-injection, and only decreased to 4.71 ± 0.27%ID/g at 120 min p.i., still 81% radioactivity retained, which demonstrated good retention in tumor throughout the process of investigation. The radioactivity of [^{18}F]1 in blood peaked at 7.00 ± 3.61%ID/g immediately at 5 min post-injection, and decreased to 3.61 ± 0.10% ID/g at 120 min post-injection. The tumor/blood uptake ratios were 0.99 at 30 min, 1.09 at 60 min and 1.3 at 120 min post-injection, and this indicated the blood clearance was not satisfactory.

For [^{18}F]**2** (Table 3), a fast clearance in liver and kidney could be observed after rapid distribution and accumulation in all organs and tissues. Radioactivity of [^{18}F]**2** in tumor was 1.40 ± 0.06, 3.32 ± 0.44, 2.98 ± 0.17 and 1.81 ± 0.13%ID/g at 5, 30, 60, and 120 min post-injection respectively, a relatively smooth trend in tumor. Surprisingly, the blood uptake reached its maximum

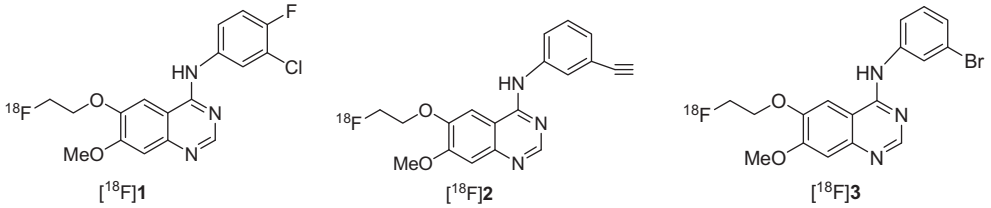

Figure 1. Structure of three ^{18}F-labeled 4-aminoquinazoline derivatives.

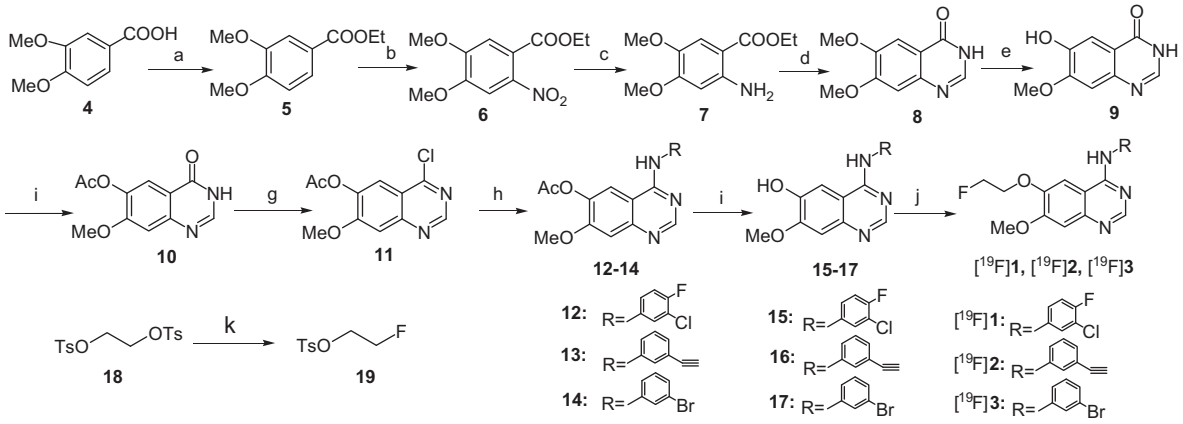

Scheme 1. Synthesis of [^{19}F]**1**, [^{19}F]**2** and [^{19}F]**3**. Experiment reagents and conditions: (a) CH_3CH_2OH, H_2SO_4, refluxing; (b) AcOH, HNO_3,0–5 °C; (c) Pd/C,H_2; (d) formamide, 160–170 °C; (e) methansulfonic acid, L-methionine, 120 °C; (f) Ac_2O, pyridine, DMAP, 100 °C; (g) $POCl_3$, toluene, refluxing; (h) R–Ar–NH2, pyridine, *i*-PrOH, refluxing; (i) NaOH, MeOH, H_2O; (j) $BrCH_2CH_2F$, K_2CO_3, DMF. (k) TBAF, CH_3CN, 90 °C.

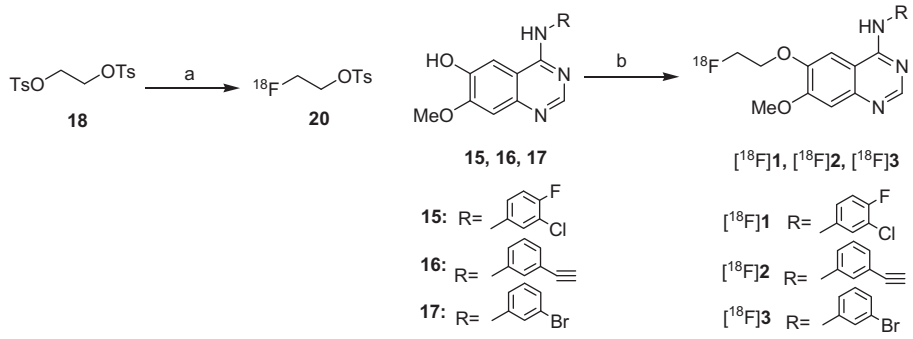

Scheme 2. Radiochemical synthesis of [^{18}F]**1**, [^{18}F]**2** and [^{18}F]**3**. Experiment reagents and conditions: (a) K^{18}F, Kryptofix 2.2.2., CH_3CN, 100 °C, 15 min; (b) intermediate **20**, KOH, DMSO, 100 °C, 15 min.

Table 1

Compounds	RCY (no decay correction)	Radio-HPLC conditions (eluent, flow rate)	Retention time
[^{18}F]**1**	21%	CH_3OH/H_2O = 80:20, 5 mL/min	8.2 min
[^{18}F]**2**	22%	CH_3OH/H_2O = 80:20, 3 mL/min	9.1 min
[^{18}F]**3**	24%	CH_3OH/H_2O = 80:20, 3 mL/min	7.3 min

Table 2
Biodistribution data of [^{18}F]**1** in mice bearing S180 tumor (%ID/g; mean ± SD; n = 4)

Organs	%ID/g ± SD			
	5 min	30 min	60 min	120 min
Heart	4.40 ± 0.02	5.02 ± 0.69	4.26 ± 0.41	2.52 ± 0.36
Liver	11.34 ± 0.79	5.38 ± 0.82	4.22 ± 0.24	2.58 ± 0.05
Spleen	4.50 ± 0.59	3.67 ± 0.55	3.23 ± 0.62	2.39 ± 0.15
Lung	4.60 ± 0.0.13	4.57 ± 0.59	3.75 ± 0.65	2.57 ± 0.21
Kidney	14.25 ± 0.98	5.20 ± 0.32	3.99 ± 0.42	2.23 ± 0.25
Stomach	5.35 ± 0.35	11.87 ± 0.49	4.44 ± 0.09	3.64 ± 0.21
Muscle	5.12 ± 0.92	4.18 ± 0.83	3.35 ± 0.73	1.74 ± 0.30
Brain	1.97 ± 0.58	3.15 ± 0.47	2.94 ± 0.14	1.98 ± 0.23
Tumor	1.87 ± 0.04	5.80 ± 0.72	5.51 ± 0.58	4.71 ± 0.27
Blood	7.00 ± 0.66	5.85 ± 0.59	5.07 ± 0.27	3.61 ± 0.10
Tumor/muscle	0.37	1.39	1.64	2.71
Tumor/blood	0.27	0.99	1.09	1.3
Tumor/brain	0.95	1.84	1.87	2.38

Table 3
Biodistribution data of [^{18}F]**2** in mice bearing S180 tumor (%ID/g; mean ± SD; n = 4)

Organs	%ID/g ± SD			
	5 min	30 min	60 min	120 min
Heart	8.68 ± 0.23	2.85 ± 0.12	1.99 ± 0.13	1.03 ± 0.08
Liver	8.75 ± 0.31	7.63 ± 0.32	4.07 ± 0.17	3.40 ± 0.09
Spleen	0.98 ± 0.15	1.93 ± 0.26	0.77 ± 0.08	1.04 ± 0.08
Lung	3.60 ± 0.14	2.99 ± 0.24	1.88 ± 0.07	1.62 ± 0.06
Kidney	6.35 ± 0.35	4.16 ± 0.31	2.53 ± 0.18	1.27 ± 0.05
Stomach	8.56 ± 0.33	5.94 ± 0.71	4.14 ± 0.38	1.07 ± 0.05
Muscle	0.74 ± 0.13	1.74 ± 0.06	0.82 ± 0.18	1.36 ± 0.12
Brain	5.51 ± 0.23	2.59 ± 0.03	0.3 ± 0.05	1.50 ± 0.04
Tumor	1.40 ± 0.06	3.32 ± 0.44	2.98 ± 0.17	1.81 ± 0.13
Blood	7.56 ± 0.36	3.06 ± 0.43	1.19 ± 0.05	0.77 ± 0.05
Tumor/muscle	1.89	1.91	3.63	1.33
Tumor/blood	0.19	1.08	2.50	2.35
Tumor/brain	0.25	1.28	9.93	1.21

7.56 ± 0.36%ID/g at 5 min, and it sharply declined to 0.77 ± 0.05%ID/g at 120 min, almost 90% radioactivity cleared from the blood. Although radioactivity in other organs and tissues presented certain uptake, it dropped faster than that in tumor as time elapsed. Therefore [^{18}F]**2** had good tumor/muscle, tumor/blood, and tumor/brain ratios at 60 min post-injection: 3.63, 2.50 and 9.93.

Table 4
Biodistribution data of [^{18}F]**3** in mice bearing S180 tumor (%ID/g; mean ± SD; n = 4)

Organs	%ID/g ± SD			
	5 min	30 min	60 min	120 min
Heart	4.79 ± 0.02	1.12 ± 0.20	0.98 ± 0.50	1.87 ± 0.59
Liver	9.67 ± 0.89	7.96 ± 0.50	1.87 ± 0.26	1.78 ± 0.34
Spleen	2.84 ± 0.52	1.25 ± 0.58	0.8 ± 0.55	1.05 ± 0.28
Lung	12.21 ± 0.52	5.12 ± 0.50	5.6 ± 0.05	3.60 ± 0.15
Kidney	10.85 ± 0.25	2.83 ± 0.14	0.90 ± 0.04	1.07 ± 0.01
Stomach	8.52 ± 0.33	7.03 ± 0.17	4.05 ± 0.06	4.10 ± 0.03
Muscle	1.87 ± 0.2	2.46 ± 0.46	0.43 ± 0.02	1.31 ± 0.12
Brain	0.78 ± 0.45	0.39 ± 0.23	0.19 ± 0.07	0.09 ± 0.01
Tumor	0.38 ± 0.02	4.04 ± 0.62	3.31 ± 0.04	3.70 ± 0.44
Blood	4.43 ± 0.46	1.58 ± 0.11	1.11 ± 0.35	0.56 ± 0.006
Tumor/muscle	0.20	1.64	7.70	2.82
Tumor/blood	0.09	2.56	2.98	6.61
Tumor/brain	0.49	10.36	17.42	41.11

As can be seen from Table 4 given below, the radioactivity accumulation of [^{18}F]**3** reached the highest level in all other organs and tissues except for muscle and tumor at 5 min post-injection. After that the radioactivity in other organs or tissues except tumor decreased, and the compound was excreted from body via kidney and liver. Maximum of radioactivity uptake in tumor was 4.04 ± 0.62%ID/g at 30 min post-injection, and decreased a little to 3.70 ± 0.44%ID/g at 120 min post-injection, still 91% radioactivity retained throughout the time course. It was obvious that [^{18}F]**3** remained a high tumor uptake level in a long period. In addition, initial radioactivity uptake in blood was 4.43 ± 0.46%ID/g, and reduced rapidly to 0.56 ± 0.006%ID/g at 120 min p.i., approximately 88% radioactivity cleared from blood. So a fast blood clearance could be seen. Since the elimination rate in tumor was much slower than that in other organs or tissues, [^{18}F]**3** had high tumor/muscle, tumor/blood, and tumor/brain ratios at 60 min post-injection: 7.70, 2.98 and 17.42.

As shown in Tables 2–4, there were some significant differences in biodistribution data of these three ^{18}F-labeled radiotracers. On the one hand, the clearance rate of [^{18}F]**3** in muscle, blood and brain was much higher than those of [^{18}F]**1** and [^{18}F]**2**. Tumor/muscle, tumor/blood, and tumor/brain ratios of [^{18}F]**3** were 7.70, 2.98 and 17.42 at 60 min post-injection, respectively. They were much higher than those of [^{18}F]**1** (1.64, 1.09 and 1.87) and [^{18}F]**2** (3.63, 2.50 and 9.93) at the same time point. On the other hand, at 60 min p.i., radioactivity uptake value of [^{18}F]**3** in tumor was 3.31, slightly higher than that of [^{18}F]**2** (2.98), less than that of [^{18}F]**1** (5.51) at the same time phase. Overall, [^{18}F]**3** among them showed the most favorable characteristics as PET tumor imaging agents: high uptake in tumor and the fastest clearance from blood and muscle. Thus, we concluded that [^{18}F]**3** was much more suitable for PET tumor imaging.

In order to determine this, we compared biodistribution data of [^{18}F]**3** with those of [^{18}F]-FDG and L-[^{18}F]-FET in the same animal model as shown in Table 5. For [^{18}F]-FDG, extremely rapid blood clearance (tumor/blood ratio was 19.47 at 60 min p.i.) and moderate clearance from muscle (tumor/muscle ratio was 2.23 at 60 min p.i.) made it widely applied in clinical as PET radiopharmaceuticals. However, its high background uptake in brain during the study period limited its application as brain tumor imaging agent. The tumor/brain uptake ratios of [^{18}F]-FDG were 0.53, 0.61, 1.02, 1.33 at 5 min, 30 min, 60 min, 120 min post-injection. For L-[^{18}F]-FET, although its tumor/blood ratios remained in a low level (1.02, 1.1 and 1.92 at 30, 60 and 120 min post-injection), higher tumor/brain ratios (2.54, 2.92 and 2.95 at 30, 60 and 120 min post-injection) enabled it to a supplement to [^{18}F]-FDG as brain imaging agents.

Compared with [^{18}F]-FDG and L-[^{18}F]-FET, [^{18}F]**3** has several distinct advantages. As shown in Table 5, absolute radioactivity uptakes of [^{18}F]**3** in tumor were higher than those of [^{18}F]-FDG and L-[^{18}F]-FET at 30, 60, 120 min post-injection. At 60 min post-injection, uptakes of [^{18}F]**3** in tumor was 3.31, which was slightly higher than those of [^{18}F]-FDG (2.16) and L-[^{18}F]-FET (2.75); [^{18}F]**3** had higher tumor/muscle uptake ratio (7.7) than those of [^{18}F]-FDG (2.3) and L-[^{18}F]-FET (1.23), which made it possible to get a clear tumor imaging for [^{18}F]**3**; It was worth mentioning that [^{18}F]**3** has a low brain uptake (0.19 ± 0.07%ID/g at 60 min p.i.) and that resulted in high tumor/brain ratio (17.42) which was ten times more than [^{18}F]-FDG (1.02) and five times more than L-[^{18}F]-FET (2.92) at 60 min post-injection; Tumor/blood uptake ratio of [^{18}F]**3** (2.98) was higher than that of L-[^{18}F]-FET (1.1), but was lower than that of [^{18}F]-FDG (19.47) at 60 min post-injection. Consequently, the described results reflected that [^{18}F]**3** could be applied in PET tumor imaging as potential tracer .

In summary, we successfully prepared three [^{18}F]-labeled 4-aminoquinazoline derivatives by two-step reaction with high yields. Biodistribution experiments of [^{18}F]**1**, [^{18}F]**2** and [^{18}F]**3** were performed in S180 tumor-bearing mice. Results indicated that [^{18}F]**3** had higher tumor/muscle uptake ratio and tumor/blood ratio than those of [^{18}F]**1** and [^{18}F]**2**. Furthermore, based upon the comparison of [^{18}F]**3** with [^{18}F]-FDG and L-[^{18}F]-FET, we found that [^{18}F]**3** had a relatively high tumor accumulation, high tumor/brain and tumor/muscle uptake ratios from 30 min onward. So [^{18}F]**3** can serve as a potential tumor imaging agent. Further research and more experiments are needed to evaluate the potential of [^{18}F]**3** and other [^{18}F]-labeled 4-aminoquinazoline derivatives to be suitable for promising PET tumor imaging radiotracers.

Table 5
Biodistribution data comparison of [^{18}F]**3**, [^{18}F]-FDG and L-[^{18}F] FET in mice bearing S180 tumor (%ID/g; mean ± SD; n = 4)[a]

Organs	Radioactive tracer	Time(min)			
		5	30	60	120
Tumor	[^{18}F]**3**	0.38 ± 0.02	4.04 ± 0.62	3.31 ± 0.04	3.70 ± 0.44
	[^{18}F]-FDG	1.27 ± 0.54	1.86 ± 0.18	2.16 ± 0.34	1.7 ± 0.06
	L-[^{18}F]-FET	2.08 ± 0.49	3.28 ± 0.69	2.75 ± 0.36	2.15 ± 1.36
Tumor/muscle	[^{18}F]**3**	0.2	1.64	7.7	2.82
	[^{18}F]-FDG	0.81	1.75	2.23	2.2
	L-[^{18}F]-FET	0.72	0.62	1.23	1.4
Tumor/blood	[^{18}F]**3**	0.09	2.56	2.98	6.61
	[^{18}F]-FDG	1.17	11.38	19.47	15.85
	L-[^{18}F]-FET	0.31	1.02	1.1	1.92
Tumor/brain	[^{18}F]**3**	0.49	10.36	17.42	41.11
	[^{18}F]-FDG	0.53	0.61	1.02	1.33
	L-[^{18}F]-FET	2.1	2.54	2.92	2.95

[a] The data of [^{18}F]-FDG and L-[^{18}F]-FET was from literature.[36]

Acknowledgments

This work was supported by National Natural Science foundation of China (No.21071022) and the Fundamental Research Funds for the Central Universities. We especially thank Ms. Man Feng for her excellent work and kindly help. We also very much appreciate the cyclotron operator team of the PET Centre of XuanWu Hospital of providing fluoride-18 nuclide and technical assistance.

Supplementary data

Supplementary data associated with this article can be found, in the online version, at http://dx.doi.org/10.1016/j.bmcl.2012.05.069.

References and notes

1. Chao, Q.; Deng, L.; Shih, H.; Leoni, L. M.; Genini, D.; Carson, D. A.; Cottam, H. B. *J. Med. Chem.* **1999**, *42*, 3860.
2. Nesterova, I. N.; Radkevich, T. P.; Granik, V. G. *Pharm. Chem. J.* **1991**, *25*, 786.
3. Nasr, M.; Drach, J. C.; Smith, S. H.; Shipman, C., Jr.; Burckhalter, J. H. *J. Med. Chem.* **1998**, *31*, 1347.
4. Mendelsohn, J.; Baselga, J. *Oncogene* **2000**, *19*, 6550.
5. Blume-Jensen, P.; Hunter, T. *Nature* **2001**, *411*, 355.
6. Lynch, T. J.; Bell, D. W.; Sordella, R.; Gurubhagavatula, S. *N. Eng. J. Med.* **2004**, *350*, 2129.
7. Morgan, M. A.; Parsels, L. A.; Kollar, L. E. *Clin Cancer Res.* **2008**, *14*, 5142.
8. László, K. *Pathol. Oncol. Res.* **2008**, *14*, 1.
9. Bonaseraa, T. A.; Ortua, G.; Rozena, Y.; Kraisa, R.; Freedmanc, N. M. T.; Chisina, R.; Gazitd, A.; Levitzki, A.; Mishania, E. *Nucl. Med. Biol.* **2001**, *28*, 359.
10. Miller, P. W.; Long, N. J.; Vilar, R.; Gee, A. D. *Angew. Chem., Int. Ed.* **2008**, *47*, 8998.
11. Wood, K. A.; Hoskin, P. J.; Saunders, M. I. *Clin. Oncol.* **2007**, *19*, 237.
12. Conti, P. S.; Lilien, D. L.; Hawley, K.; Keppler, J.; Grafton, S. T.; Bading, J. R. *Nucl. Med. Biol.* **1996**, *23*, 717.
13. Laverman, P.; Boerman, O. C.; Corstens, F. H. M.; Oyen, W. J. *Eur. J. Nucl. Med.* **2002**, *29*, 681.
14. Varagnolo, L.; Stokkel, M. P. M.; Mazzi, U.; Pauwels, E. K. *Nucl. Med. Biol.* **2000**, *27*, 103.
15. Wester, H. J.; Herz, M.; Weber, W.; Heiss, P.; Senekowitsch-Schmidtke, R.; Schwaiger, M.; Stocklin, G. *J. Nucl. Med.* **1999**, *40*, 205.
16. Bonasera, T. A.; Ortu, G.; Rozen, Y. *Nucl. Med. Biol.* **2001**, *28*, 359.
17. Seimbille, Y.; Phelps, M. E.; Czernin, J.; Silverman, D. H. S. *J. Labelled Compd. Radiopharm.* **2005**, *48*, 829.
18. Su, H.; Seimbille, Y.; Ferl, G. Z.; Bodenstein, C.; Fueger, B.; Kim, K. J.; Hsu, Y.-T.; Phelps, M. E.; Czernin, J.; Weber, W. A. *Eur. J. Nucl. Med. Mol. Imaging* **2008**, *1089*, 35.
19. Fredriksson, A.; Johnström, P.; Thorell, J.-O.; von Heijne, G.; Hassan, M.; Eksborg, S.; Kogner, P.; Borgström, P.; Ingvar, M.; Stone-Elander, S. *Life Sci.* **1999**, *65*, 165.
20. Bridges, A. J.; Zhou, H.; Cody, D. R.; Rewcastle, G. W.; McMichael, A.; Showalter, H. D.; Fry, D. W.; Kraker, A. J.; Denny, W. A. *J. Med. Chem.* **1996**, *39*, 267.
21. Mishani, E.; Abourbeh, G. *Curr. Top Med. Chem.* **2007**, *7*, 1755.
22. Mishani, E.; Hagooly, A. *J. Nucl. Med.* **2009**, *50*, 1199.
23. Pal, A.; Balatoni, J. A.; Mukhopadhyay, U.; Ogawa, K.; Gonzalez-Lepera, C.; Shavrin, A.; Volgin, A.; Tong, W.; Alauddin, M. M.; Gelovani, J. G. *Mol. Imaging Biol.* **2011**, *13*, 853.
24. Su, H.; Seimbille, Y.; Ferl, G. Z.; Bodenstein, C.; Fueger, B.; Kim, K. J.; Hsu, Y. T.; Dubinett, S. M.; Phelps, M. E.; Czernin, J.; Weber, W. A. *Eur. J. Nucl. Med. Mol. Imaging.* **2008**, *1089*, 35.
25. Holt, D. P.; Ravert, H. T.; Dannals, R. F.; Pomper, M. G. *J. Labelled Compd. Radiopharm.* **2006**, *49*, 883.
26. Memon, A. A.; Jakobsen, S.; Dagnaes-Hansen, F.; Sorensen, B. S.; Keiding, S.; Nexo, E. *Cancer Res.* **2009**, *69*, 873.
27. Ortu, G.; Ben-David, I.; Rozen, Y.; Freedman, N. M.; Chisin, R.; Levitzki, A.; Mishani, E. *Int. J. Cancer.* **2002**, *101*, 360.
28. Mishani, E.; Abourbeh, G.; Rozen, Y.; Jacobson, O.; Laky, D.; Ben David, I.; Levitzki, A.; Shaul, M. *Nucl. Med. Biol.* **2004**, *31*, 469.
29. Abourbeh, G.; Dissoki, S.; Jacobson, O.; Litchi, A.; Ben Daniel, R.; Laki, D.; Levitzki, A.; Mishani, E. *Nucl. Med. Biol.* **2007**, *34*, 55.
30. Bridges, A. *J. Chem. Rev.* **2001**, *101*, 2541.
31. Knesl, P.; Röseling, D.; Jordis, U. *Molecules* **2006**, *11*, 286.
32. Ban, H. S.; Tanaka, Y.; Nabeyama, W.; Hatori, M.; Nakamura, H. *Bioorg. Med. chem.* **2010**, *18*, 870.
33. Cai, X.; Zhai, H. X.; Wang, J.; Forrester, J.; Qu, H.; Yin, L.; Lai, C. J.; Bao, R.; Qian, C. *J. Med. Chem.* **2000**, *2010*, 53.
34. Chandregowda, V.; Kush, A. K.; Reddy, G. C. *Eur. J. Med. Chem.* **2009**, *44*, 3046.
35. Qiao, Y.; He, Y.; Zhang, S.; Li, G.; Liu, H.; Xu, J.; Wang, X.; Qi, C.; Peng, C. *Bioorg. Med. Chem. Lett.* **2009**, *19*, 4873.
36. Zhang, S.; Wang, X.; He, Y.; Ding, R.; Liu, H.; Xu, J.; Feng, M.; Li, G.; Wang, M.; Peng, C.; Qi, C. *Bioorg. Med. Chem. Lett.* **2009**, *19*, 4873.